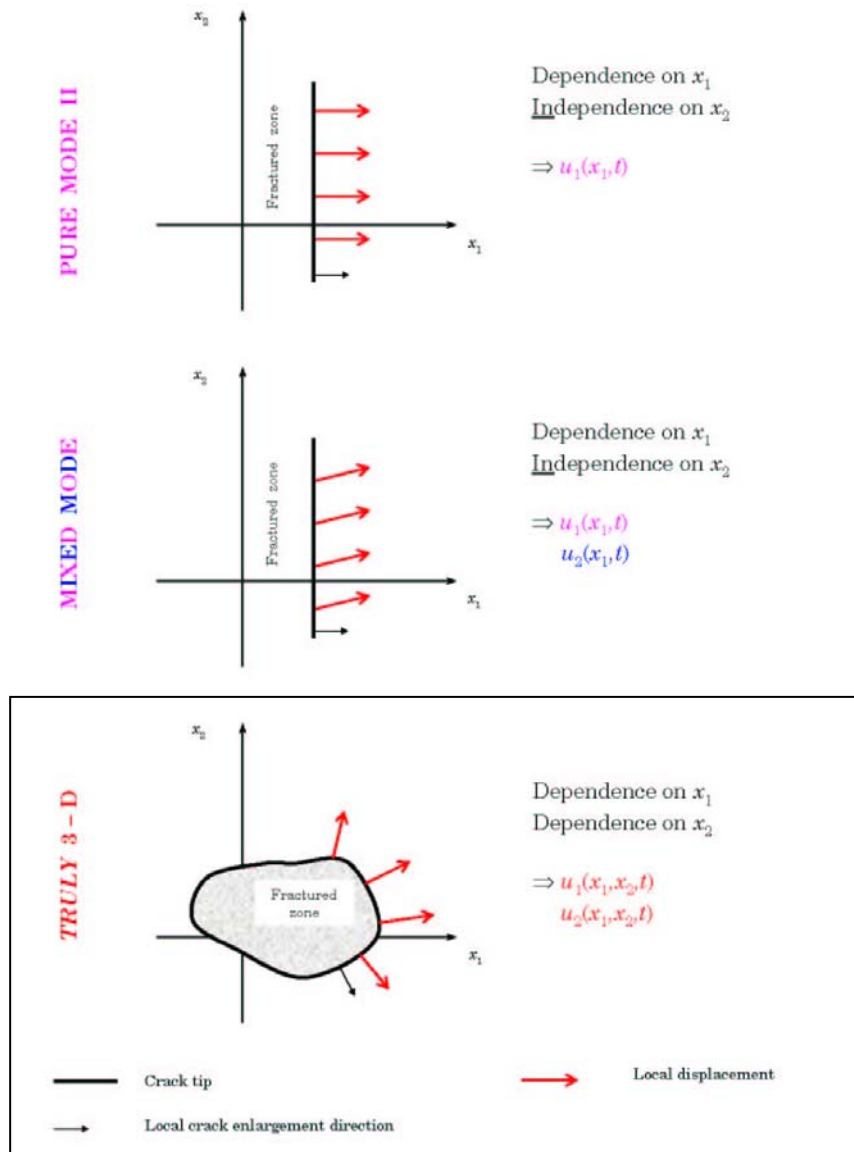




Rupture propagation in
a *truly* 3 – D fault model



Remembering dimensionality ...

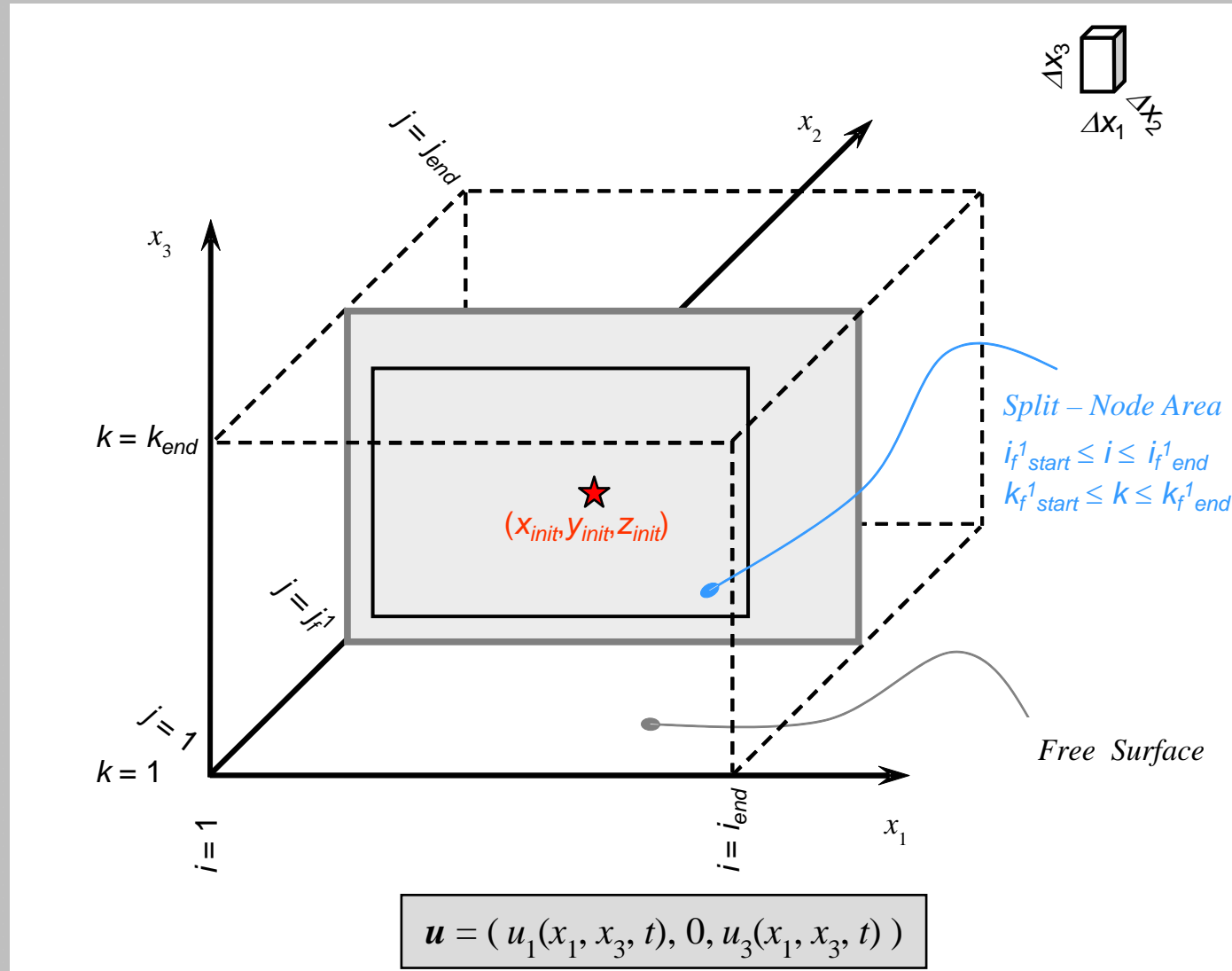


We solve a *truly* 3 – D rupture problem:

- Both two components of solutions depend on two spatial coordinates and on time;
- Shear traction is collinear with fault slip velocity ($T // v$), but the rake (i. e. the fault slip velocity azimuth) can vary during time.



Numerical Method: FD 3 - D





In the assumed fault geometry, on a **generic fault point** (defined by the absolute coordinate (x_1, x_2^f, x_3)), at time t , the traction vector is:

$$\mathcal{T} = (\sigma_{21}, -\sigma_n^{eff}, \sigma_{23})$$

where:

$\sigma_n^{eff} = \sigma_n - p_{fluid}$ effective normal stress (normal stresses are negative for compression)

$\sigma_n = -\sigma_{22}$ is the regional normal stress (e. g. lithostatic stress: $\sigma_{22} = -p_0 \delta_{22} = -\rho g x_3$)

σ_{21}, σ_{23} (shear stresses, associated to the adopted fault constitutive law)



In the assumed fault geometry, on a **generic medium point** (defined by the absolute coordinate (x_1, x_2, x_3)), at time t , the stress tensor matrix is:

$$\sigma_{ij}(x_1, x_2, x_3, t) = \lambda e_{kk}(x_1, x_2, x_3, t) \delta_{ij} + 2\mu e_{ij}(x_1, x_2, x_3, t)$$

(i. e. the Hooke' s law for a linealry homogeneous, isotropic medium, within the small displacement approximation)

where:

$$e_{ij} = \frac{1}{2} (U_{i,j} + U_{j,i})$$

is calculated from the displacement field \mathbf{U} , generated by the rupture propagation on the fault surface Σ .



The FD_3D Numerical Code

We solve the fundamental elastodynamic equation, neglecting body forces \mathbf{f}

$$\rho \ddot{\mathbf{U}}_i = \sigma_{ijj} + f_i$$

A mathematical equation is shown, crossed out with a large red X. The equation is $\rho \ddot{\mathbf{U}}_i = \sigma_{ijj} + f_i$, where ρ is density, $\ddot{\mathbf{U}}$ is acceleration, σ is stress, and f is body force.

We discretize the volume in $x_1x_2x_3$ space by using cubic building blocks. The space is linearly elastic except that in **6 planes**, representing 4 dipping and 2 vertical faults

Displacements, forces and tractions are staggered in time with respect to the slip velocity components

An explicit displacement discontinuity is assumed between the two sides of faults: **Traction – at – Split – Node** scheme

We take into account the **rake rotation** during propagation: the rake direction is calculated from fault strength.

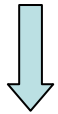


The code is based on **Dynelf** by D. J. Andrews ([nearly 1623 F77 code lines](#)):

- **2n – order** in space and in time;
- FE scheme with **specialized elements**: the discretization is made by using the quadrilateral isoparametric elements (Hughes, 1987) with all edges parallel to the axes of the Cartesian coordinate system;
- **planar free surface**;
- finite differences in space are formulated to be equivalent to finite elements and therefore the numerical algorithm can be considered either as a Finite Element or as a Finite Difference scheme;
- the formulation is mathematically equivalent to the local stiffness matrix, but it is more efficient;
- the main physical quantities are **updated explicitly through time**;
- the fundamental physical variables are **displacement** and **force** at nodes;
- local forces are calculated using the 8-points Lobatto integration;
- stress is not uniform inside an element.

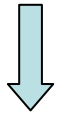


- Conventional – grid based code;
- Displacement components (U_i)



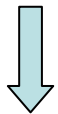
Strain rate components (e_{ij})

small displacement approximation



Stress tensor components (σ_{ij})

Hooke law for isotropic medium



Local force components (F_i)

II law of dynamic



Acceleration components (A_i)

by defintion



Updated displacement and displacement rate components (U_i^{new} , V_i^{new});

- \mathbf{U} is known at half – integer time levels; other quantities at integer time levels.



The code has been modified (now is more than 11,000 lines) to include:

- 1) Different governing laws (including rate – and state – dependent friction laws) using an accurate Fault Boundary Condition and accounting for spatial heterogeneities of the constitutive parameters. Rake can vary during time;
- 2) The implementation of thermal pressurization model and variation of the effective normal stress with time;
- 3) Various nucleation strategies to force the rupture to propagate;
- 4) Absorbing Boundary Conditions in order to eliminate reflections from the domain boundaries and to drastically reduce the computational requests (RAM and CPU time);
- 5) Computational optimization (loop unroll and routine inline), in collaboration with Thomas Schoenemeyer of NEC;
- 6) Calculation of rupture times on the fault and seismic moment. Outputting of arbitrary numbers of time snapshots of all relevant quantities on the fault and in the surrounding medium



- Dynamic loads at time t , in each node of the fault plane (Σ):

$$\mathcal{L}_i = f_{ri} + T_{0i} \quad (i = 1 \text{ and } 3).$$

where:

f_{ri} are the components of the load (restoring forces per unit fault area, f_r) exerted by the neighboring points of the fault; $f_{ri} = (M^-f_i^+ - M^+f_i^-)/[\mathcal{A}(M^+ + M^-)]$, with M^+ and M^- are the masses of the “+” and “-” half split-node of the fault plane S (see Figure 2b) and f^+ the force per unit fault area acting on partial node “+” caused by deformation of neighbouring elements in the “-” side of Σ .

T_{0i} are the components of the initial shear traction

- Component of fault traction T_i are calculated solving the coupled equations

$$\frac{d^2}{dt^2} u_1 = \alpha [\mathcal{L}_1 - T_1]$$
$$\frac{d^2}{dt^2} u_3 = \alpha [\mathcal{L}_3 - T_3]$$

where: $\alpha \equiv \mathcal{A} ((1/M^+) + (1/M^-))$, \mathcal{A} being the split-node area (in the case of vertical fault $x_2 = x_2^f$ is: $\mathcal{A} = \Delta x_1 \Delta x_3$)



- Components of the shear traction are coupled through the **boundary condition**

$$T = \tau$$

where:

$$T = \sqrt{T_1^2 + T_3^2}$$

τ is the analytical expression of the **governing law** (namely the fault strength)

- The latter depends on the effective normal stress

$$\sigma_n^{eff} = - (\Sigma^{(\hat{n})} \cdot \hat{n} + p_{fluid})$$

where:

$\Sigma^{(\hat{n})} \cdot \hat{n}$ is the **normal stress** acting on the solid matrix

p_{fluid} is the **pore fluid pressure**.

A time t is:

$$\sigma_n^{eff}(x_1, x_3, t) = - f_{r2} + \sigma_n^{eff}(x_1, x_3, 0)$$



Reference Case



Slip

Traction

Slip_26ani_sw_total

$S = 0.8$
In. rake = 0.785398 rad.

Tau_26ani_sw_total

$S = 0.8$
In. rake = 0.785398 rad.

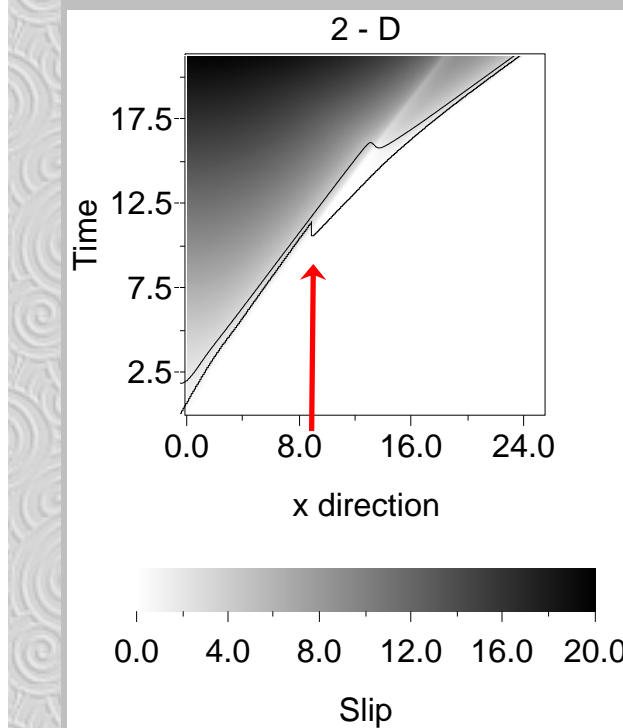
Anim_Slip_26ani_sw_total.avi

Anim_Tau_26ani_sw_total.avi

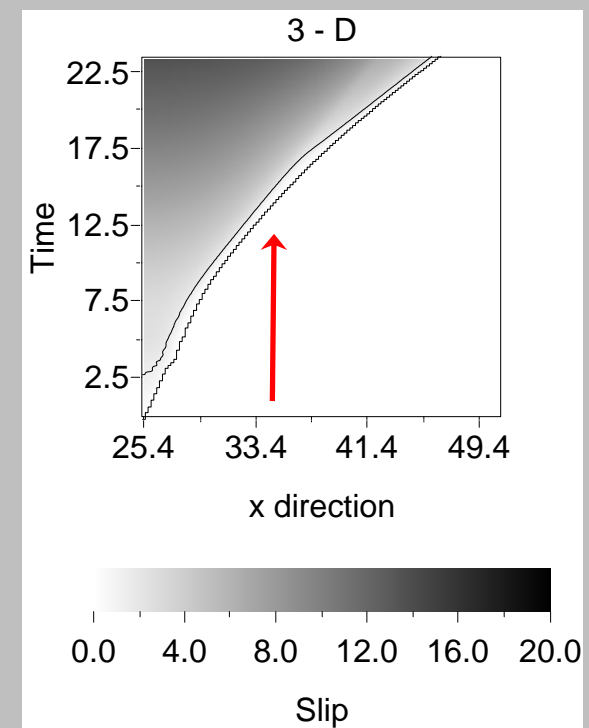
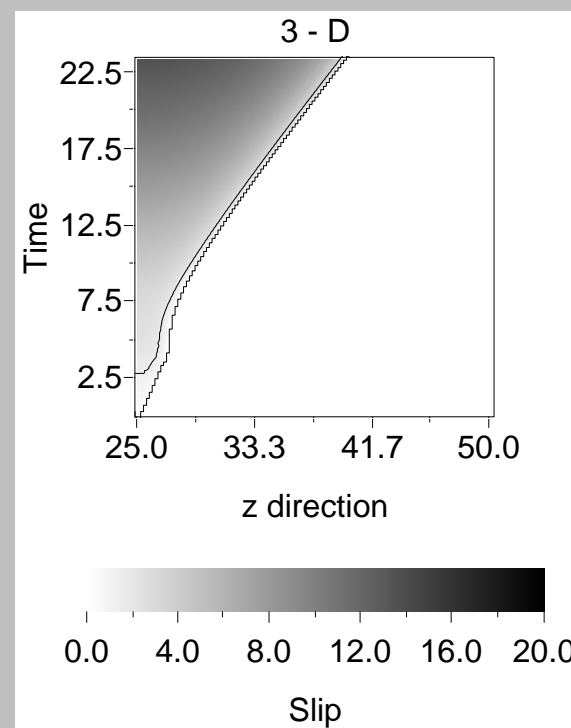


Comparision between 2 - D and 3 - D models #1

Fixed x_1 coordinate

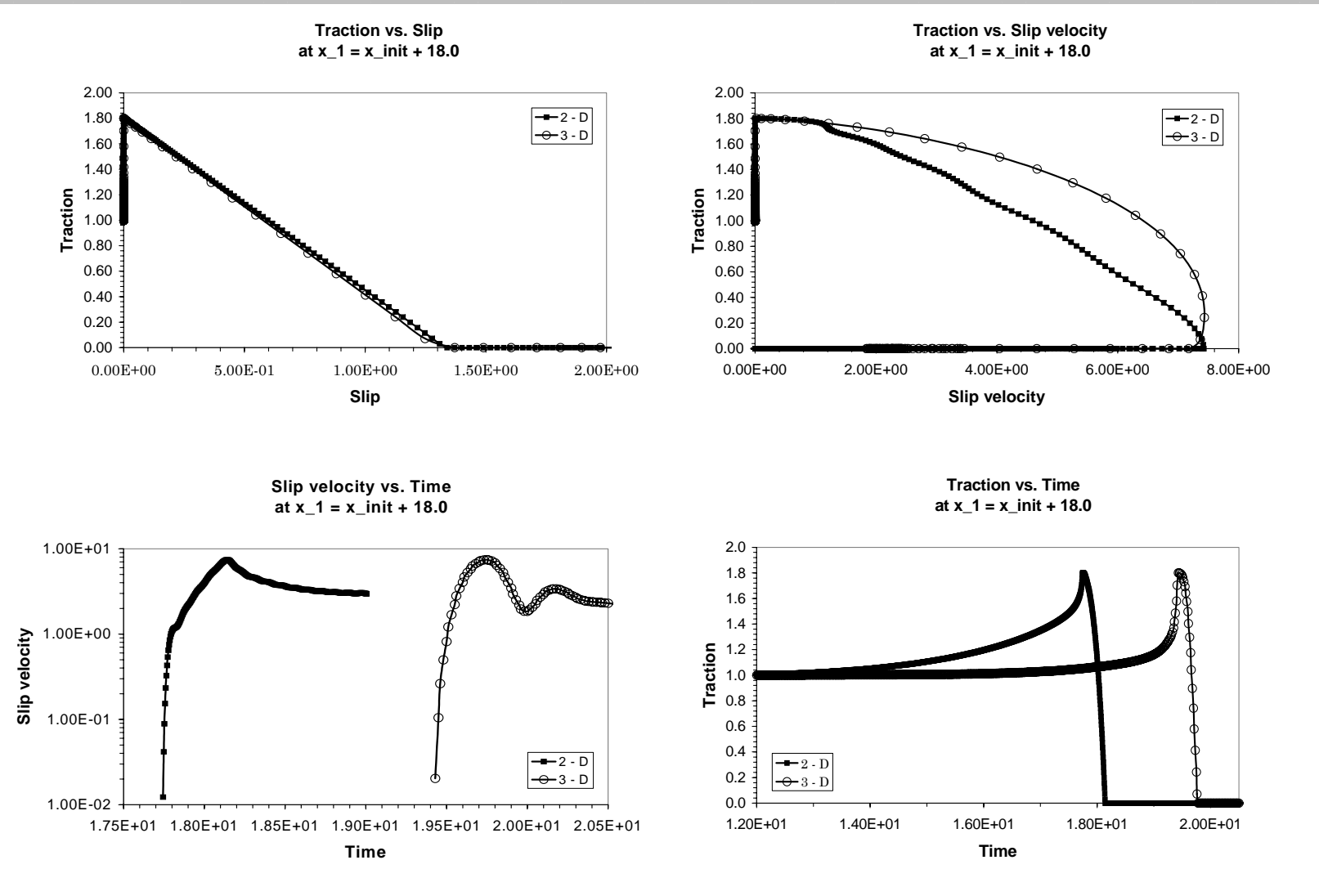


Fixed x_3 coordinate



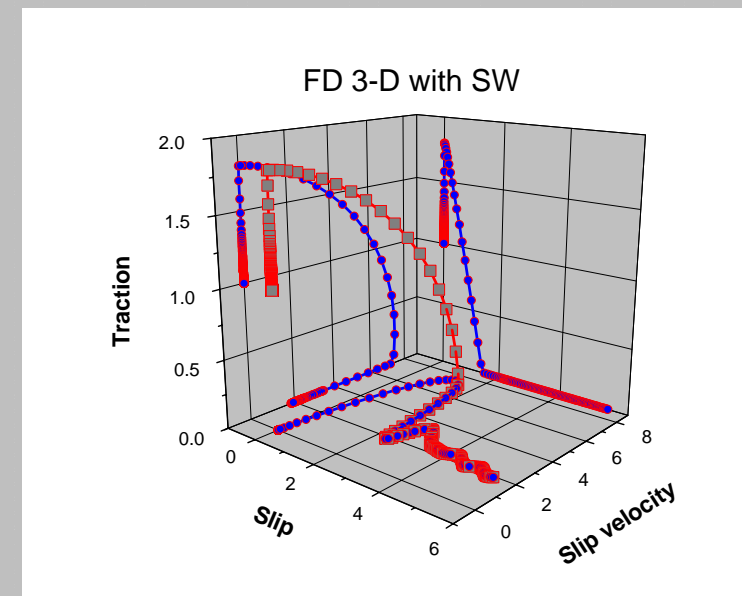
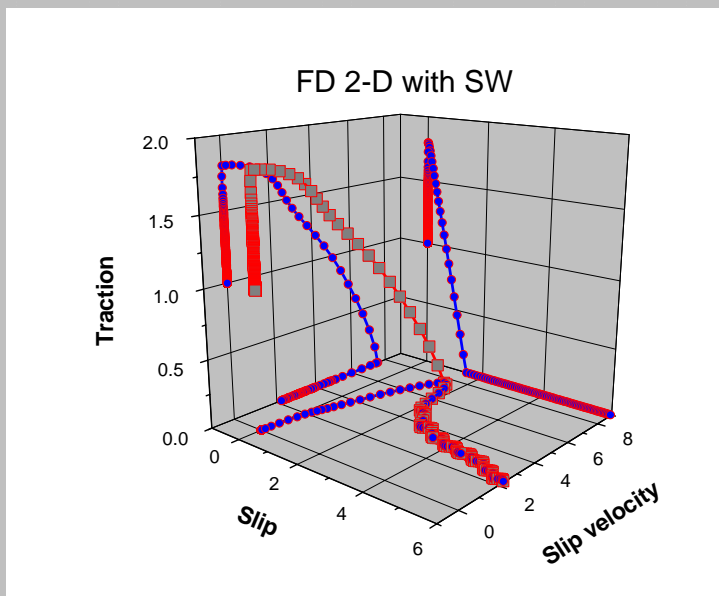
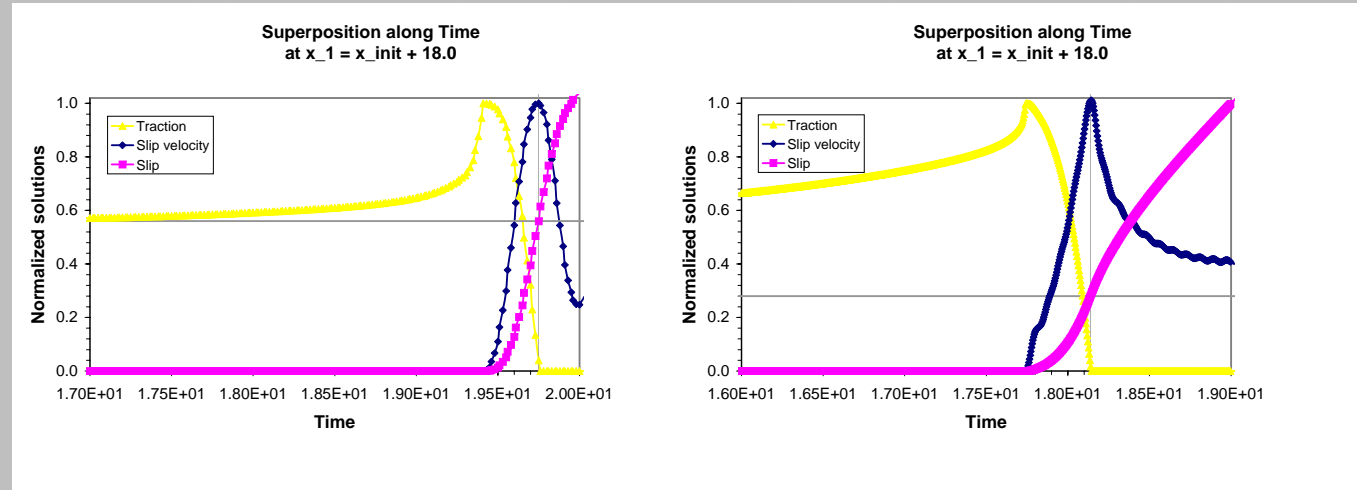


Comparision between 2 - D and 3 - D models #2



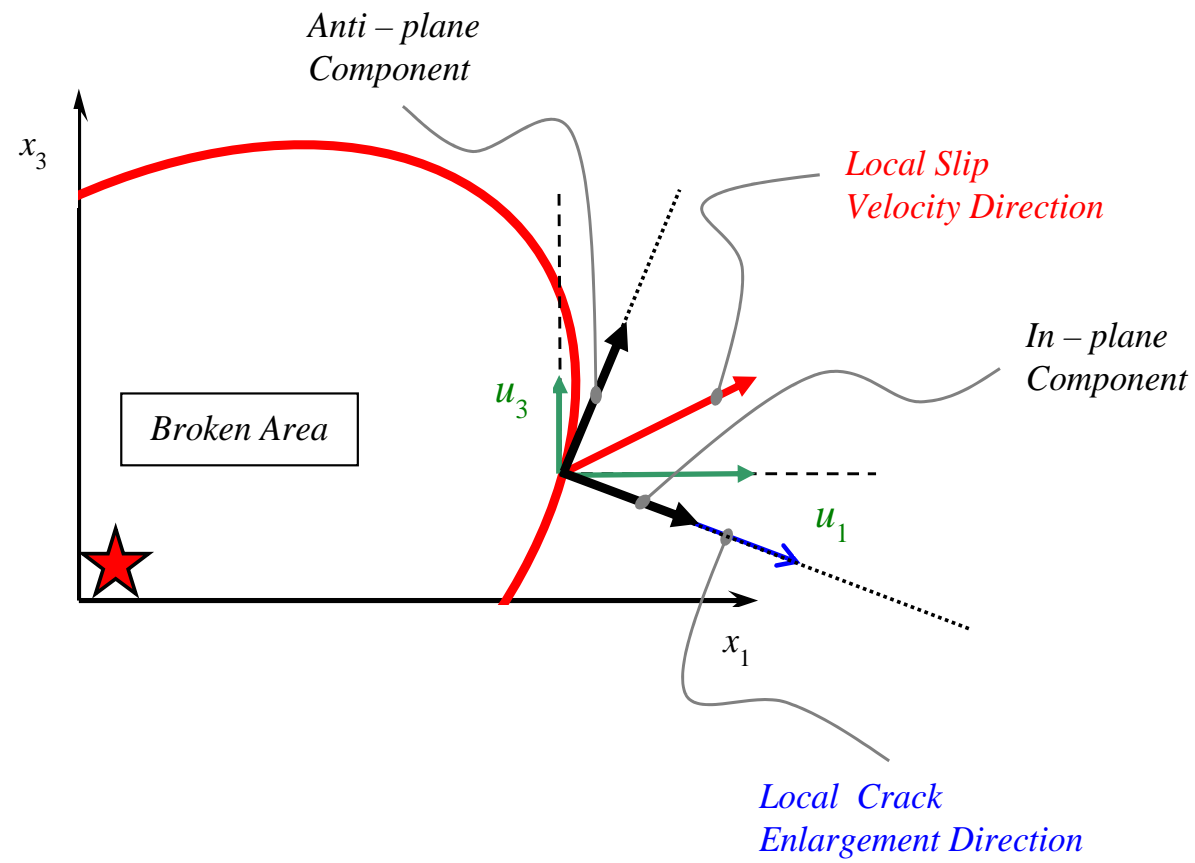


Comparision between 2 - D and 3 - D models #3





The rake rotation: the coupling of the two modes of propagation



Rake rotation #1: Theoretical background

- In the case of **self – similar**, expanding **elliptical cracks** the slip is **everywhere parallel** to the direction of pre – stress, even in the extreme situation of zero friction (*Burridge and Willis, 1969*).
- In the case of a **finite circular crack** *Madariaga (1976)* showed that rupture introduces a **component perpendicular** to the direction of pre – stress, which is quite small.
- The rake rotation is, by defintion, **explicitely neglected** in fault models where the pre – stress is assumed parallel to one coordinate axis and the slip is **not** allowed in the direction perpendicular to the pre – stress (*Aochi et al., 2000a, 2000b; Fukuyama and Madariaga, 2000; Madariaga et al., 1998; Nielsen and Olsen, 2000*) ...
... as well as in models where the governing law is assumed in a vectorial form (i. e. independently for each components of physical observables), but only one component is non null (*Fukuyama and Madariaga, 1998; Fukuyama et al., 2003; Olsen et al., 1997*).

Rake rotation #2: evidences

From Spudich et al., (1998)

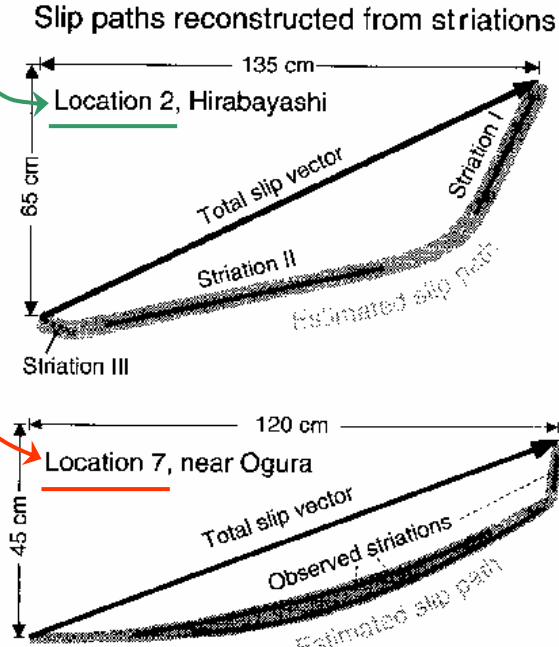


Figure 2. Black lines: striations observed at locations 2 and 7. Gray bands: slip paths inferred from striation locations 2 and 7. From Otsuki et al. (1997).

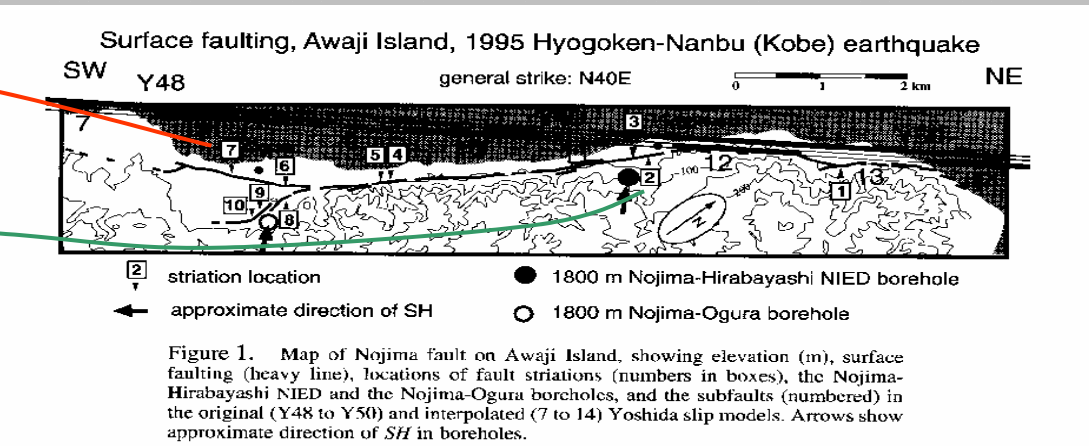


Figure 1. Map of Nojima fault on Awaji Island, showing elevation (m), surface faulting (heavy line), locations of fault striations (numbers in boxes), the Nojima-Hirabayashi NIED and the Nojima-Ogura boreholes, and the subfaults (numbered) in the original (Y48 to Y50) and interpolated (7 to 14) Yoshida slip models. Arrows show approximate direction of SH in boreholes.

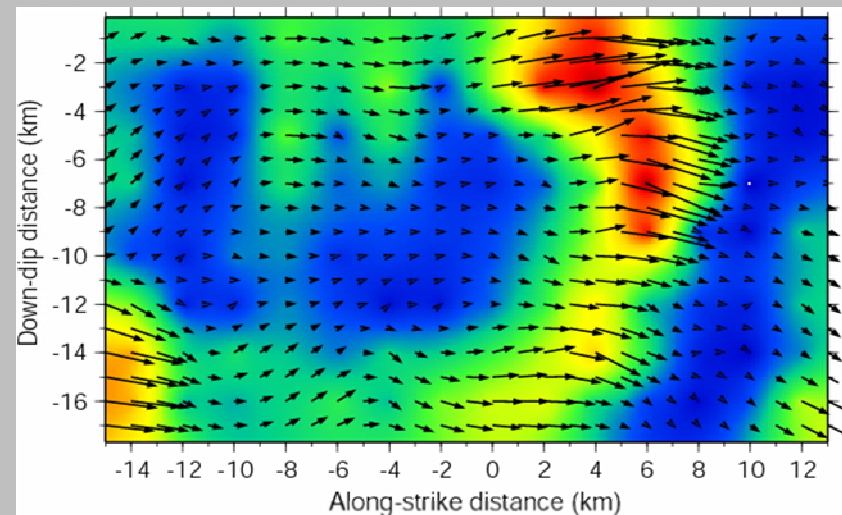
Etchecopar (1984), Florensov and Solonenko (1965), Kakimi et al. (1977), Philip and Megard (1977).

More recently curved striations (also called slickenlines) were seen in the Denali earthquake (Haeussler et al. 2004).

Curved striations were observed in the 1971 San Fernando; 1999 Hector Mine EQ; the 1992 Landers EQ; the 1980 El Asnam, Algeria EQ, and on the San Andreas in the Mecca Hills.

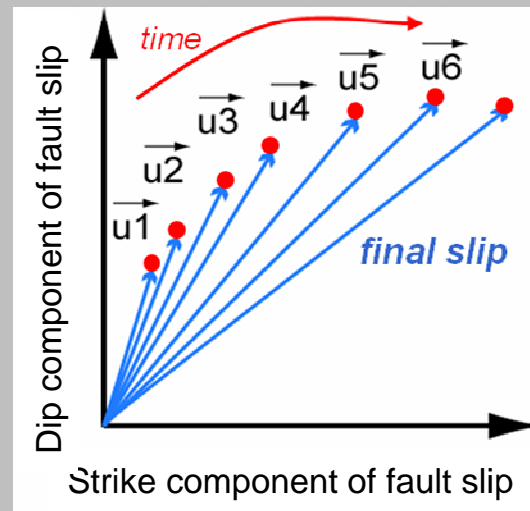
Rake rotation: a schematic example

Spatial heterogeneous rake

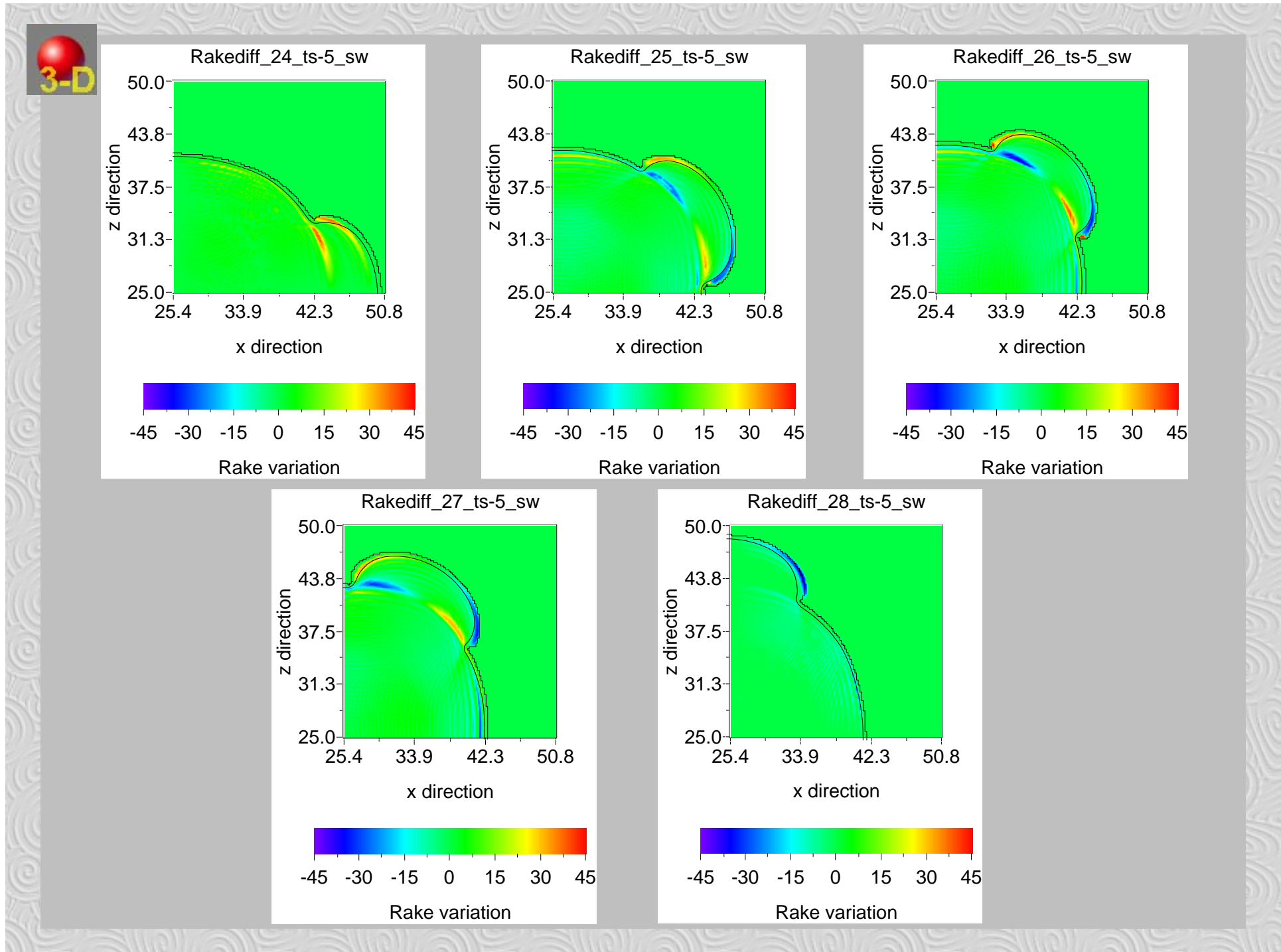


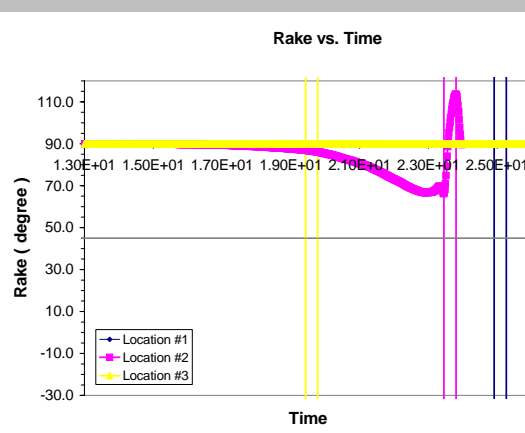
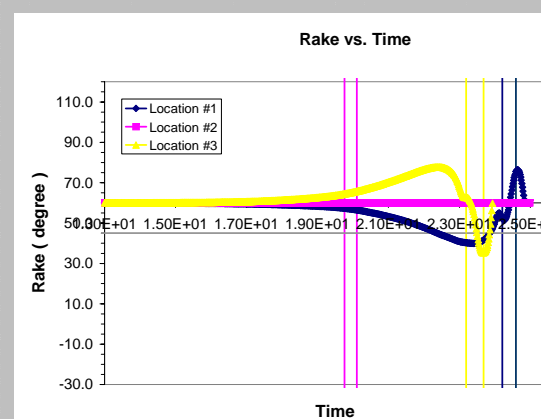
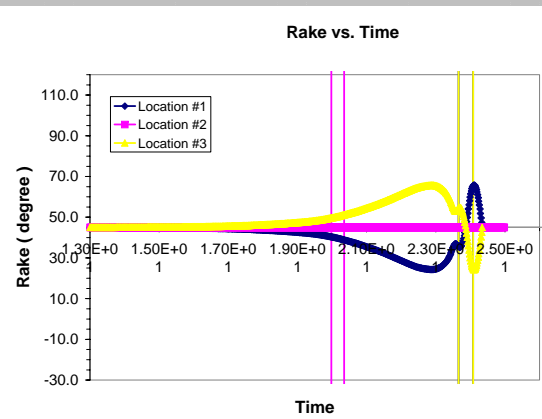
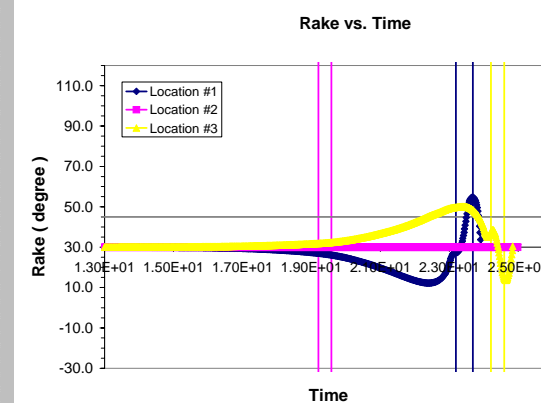
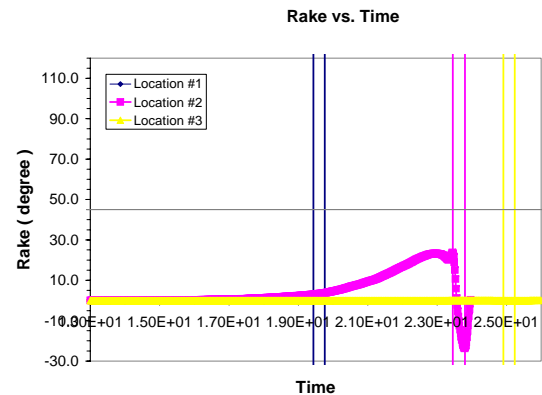
Slip distribution on the fault

Temporal heterogeneous rake



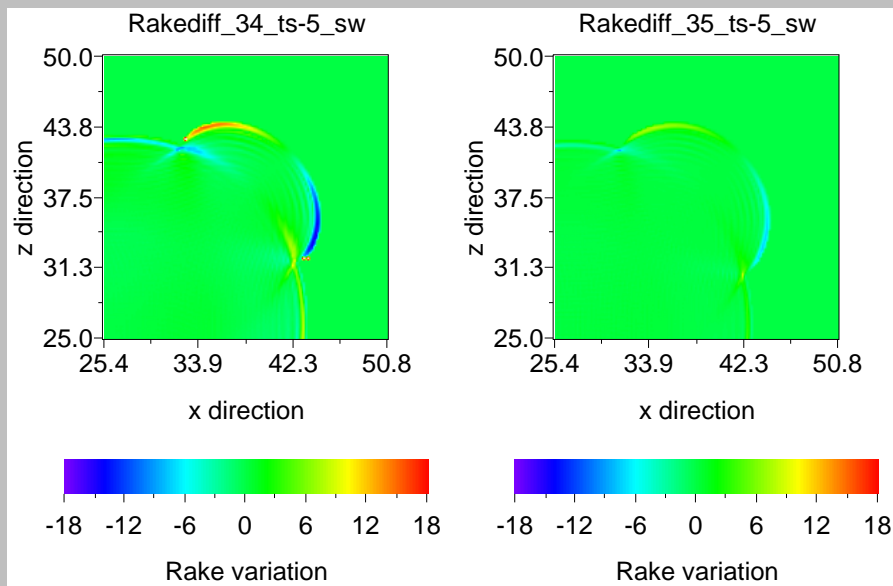
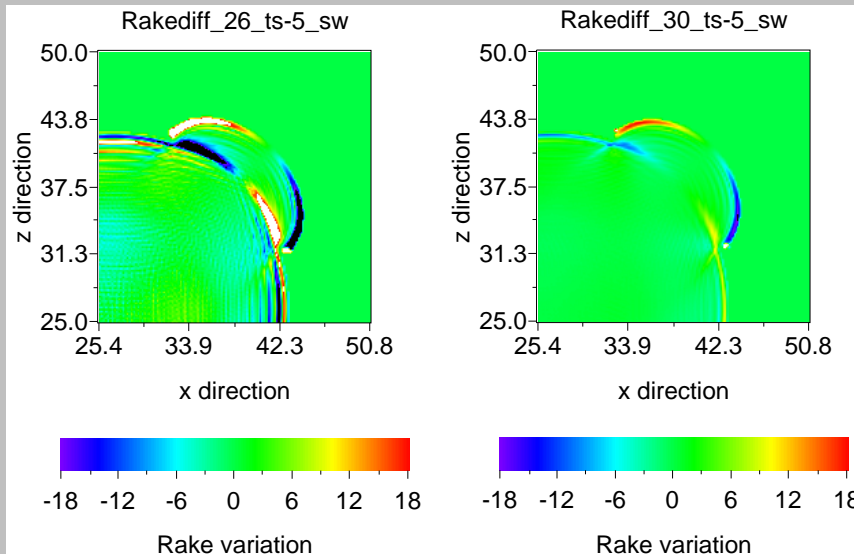
Temporal evolution of slip for a target point





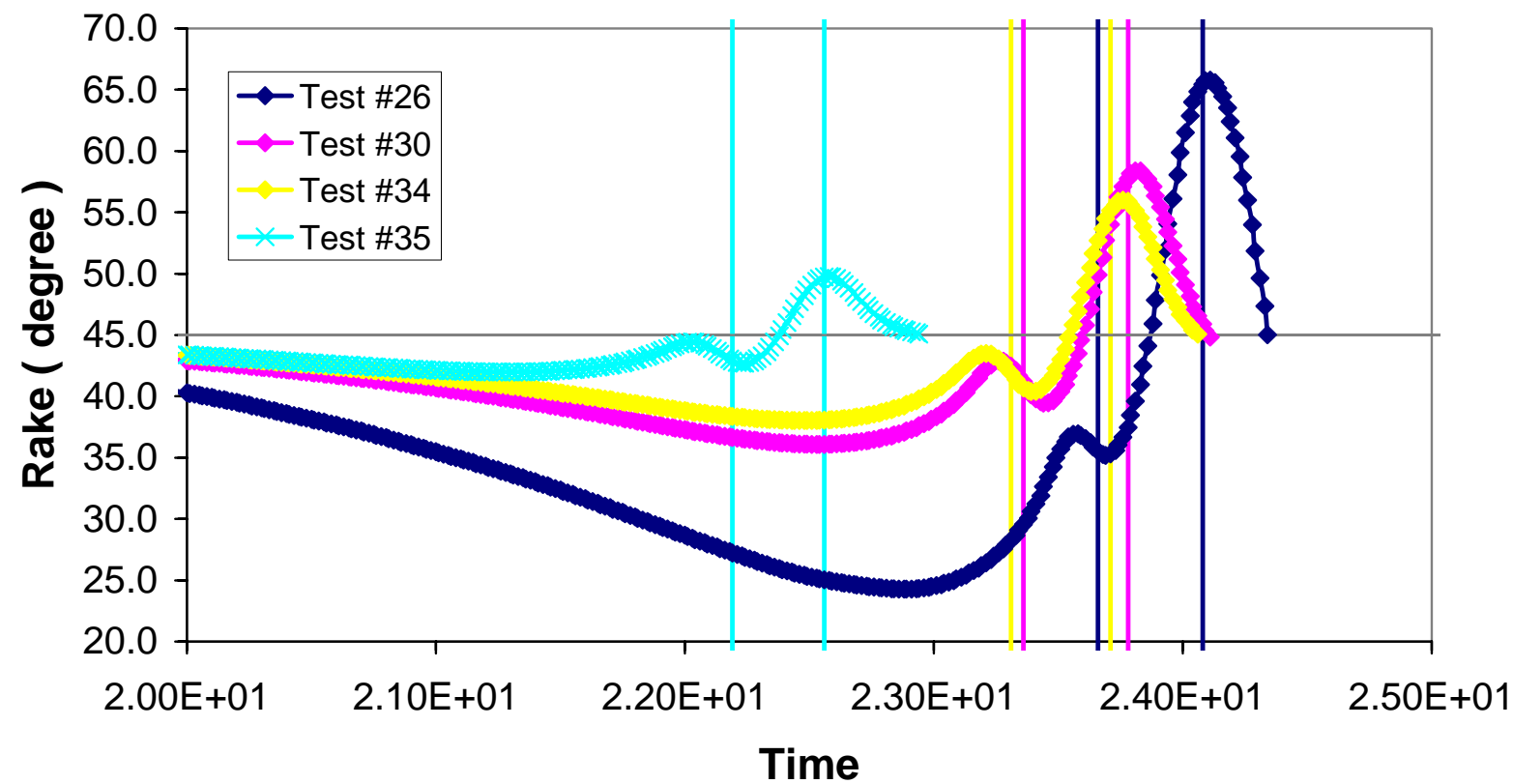


Rake rotation #4: dependence on the absolute stress level



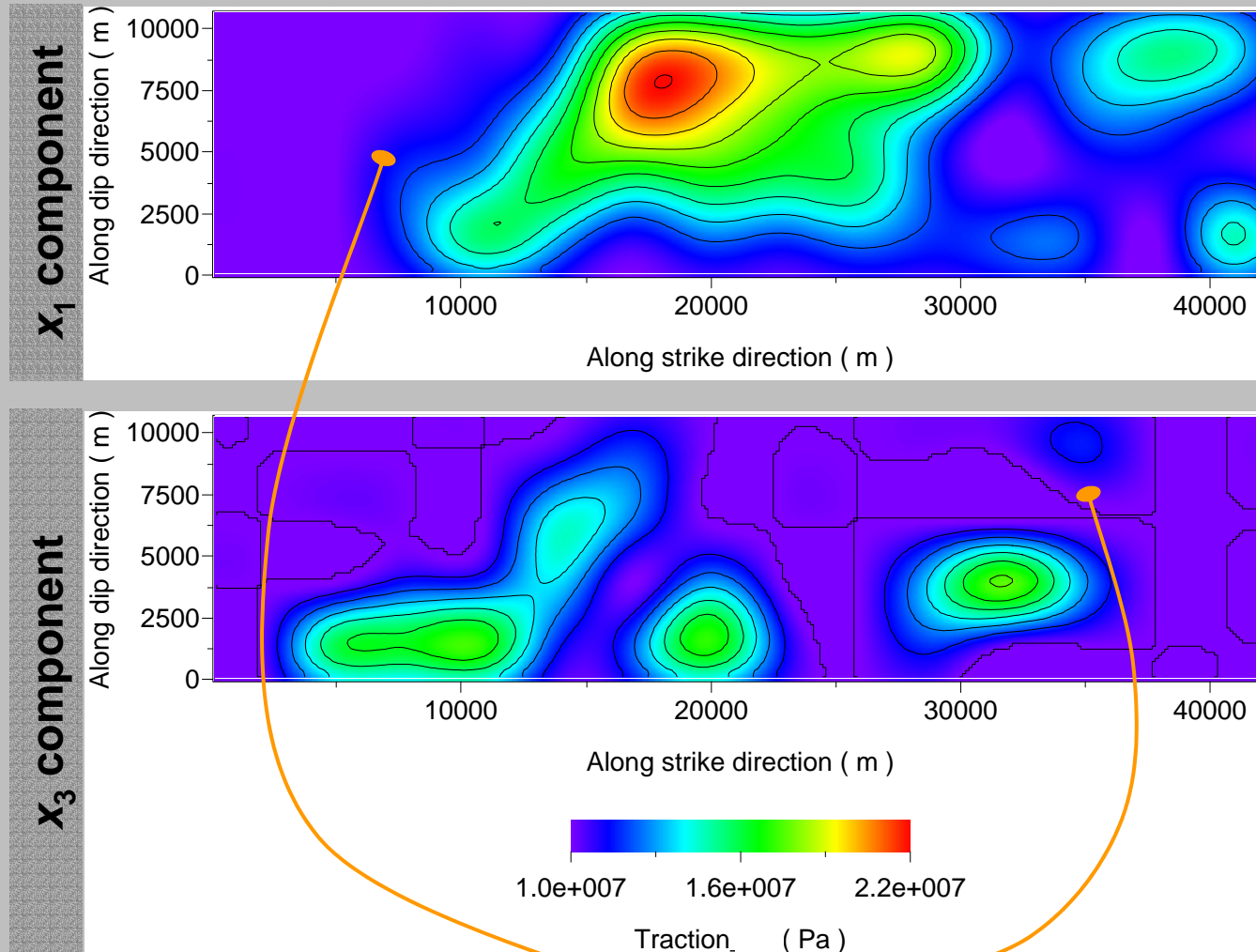


Rake vs. Time
 $\text{dist} = r_{\text{init}} + 18.0$
Location #1





The rake rotation #5: path / modulus



$$\mathbf{T}_0(x_1, x_3) \equiv \mathbf{T}(x_1, x_3, 0) = (T_1(x_1, x_3, 0), 0, T_3(x_1, x_3, 0))$$

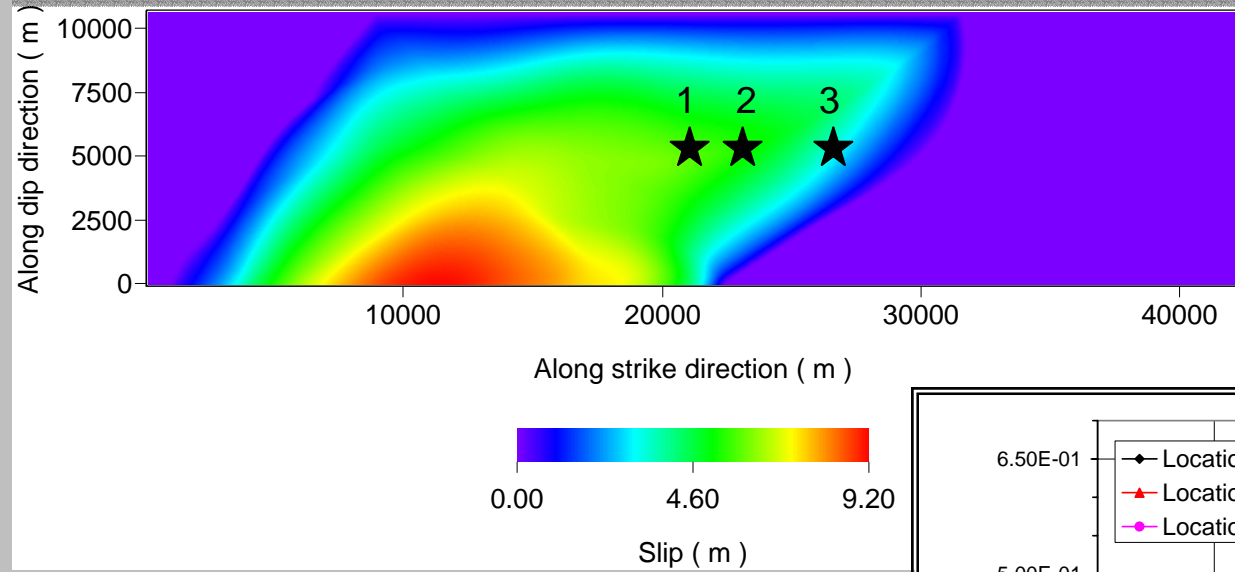
Normal Traction $\rightarrow \Sigma_0(x_1, x_3) \equiv \Sigma(x_1, x_3, 0) = -\sigma_n^{eff} \hat{\mathbf{n}} = (0, -30 \text{ MPa}, 0)$

$$T_0 = \mathbf{T}_0 + \Sigma_0$$

Total Traction



Fault slip time snapshots – Linear SW assumed

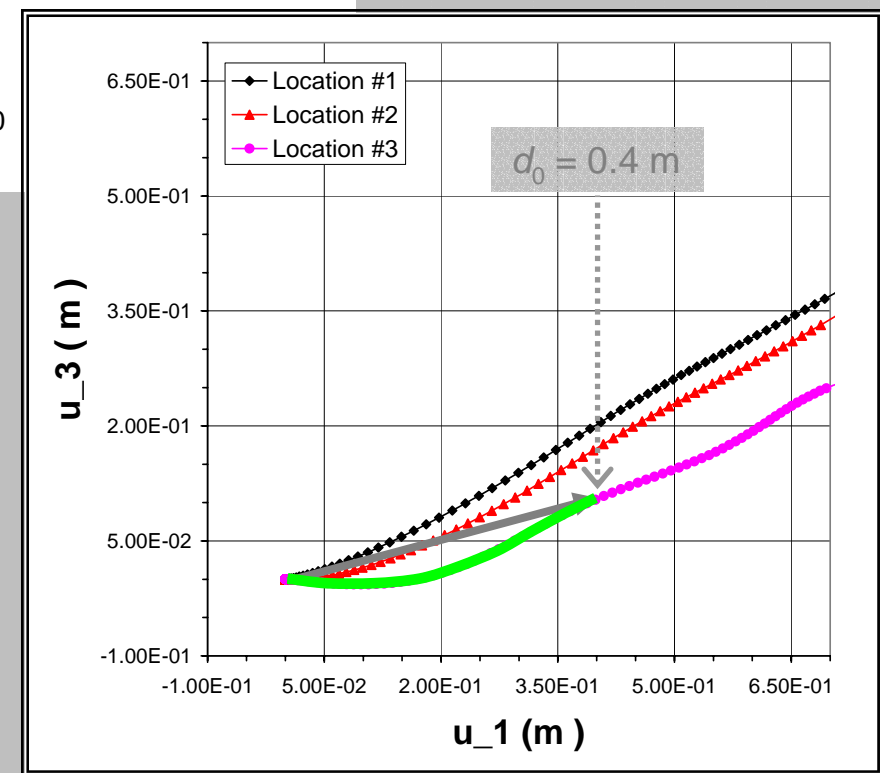


Slip modulus:

$$u = u^{(mod)}(x_1, x_3, t) \equiv \| \mathbf{u}(x_1, x_3, t) \|$$

Slip path:

$$u = u^{(path)}(x_1, x_3, t) \equiv \int_0^t \| \mathbf{v}(x_1, x_3, t') \| dt'$$



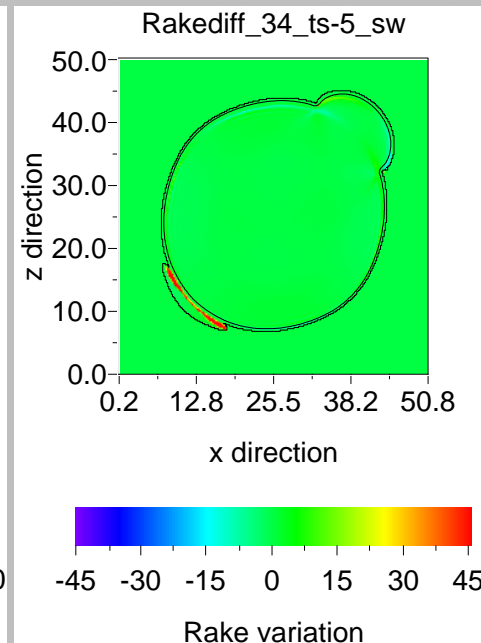
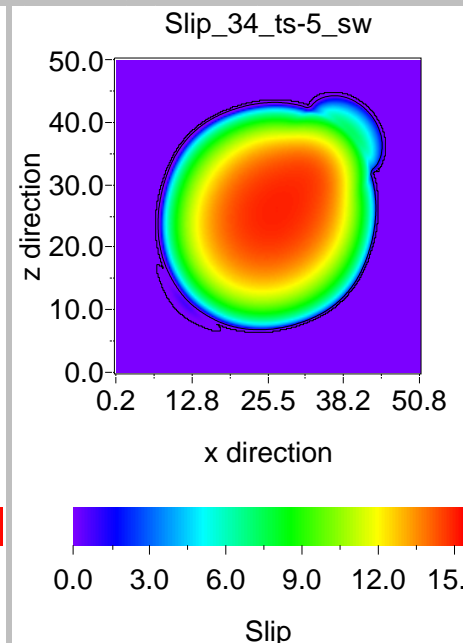
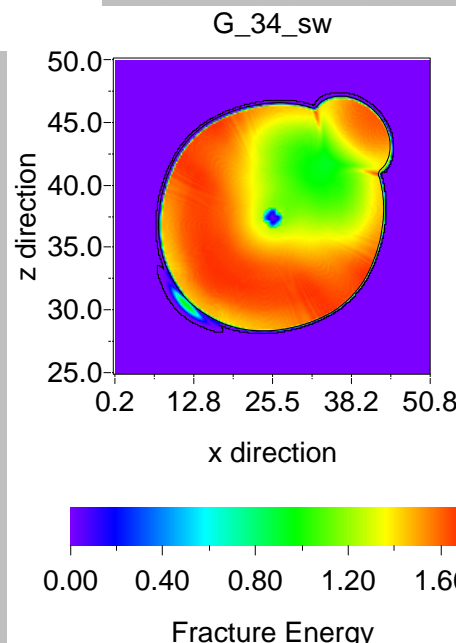
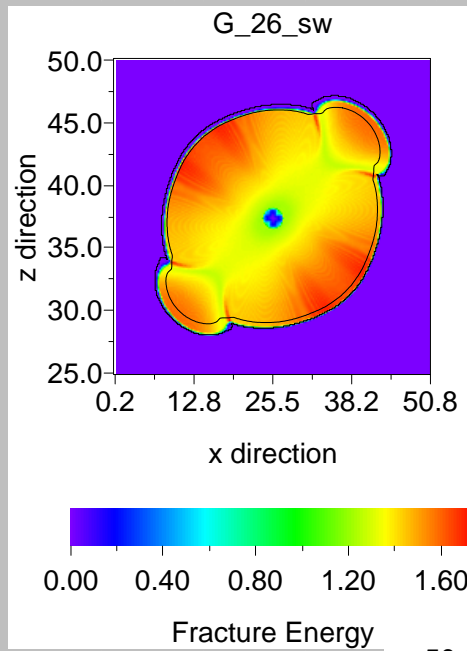
The ambiguity between modulus and path exists only for governing laws containing a dependence on *fault slip* (for instance in the case of rate – and state – dependent friction there is no other possibility than modulus of fault slip velocity).

In the papers taking into account both components of fault slip (and fault slip velocity and fault traction)

- *Bizzarri and Belardinelli (2007); Bizzarri and Cocco (2005, 2006a, 2006b); Bizzarri and Spudich (2007); Olsen et al. (1997)* considered the dependence on slip modulus;
- *Dalguer and Day (2006); Day et al., (1982a, 1982b); Day et al. (2005)* considered the dependence on *slip path*.



Effect of the free surface



Slip complexity and heterogeneities

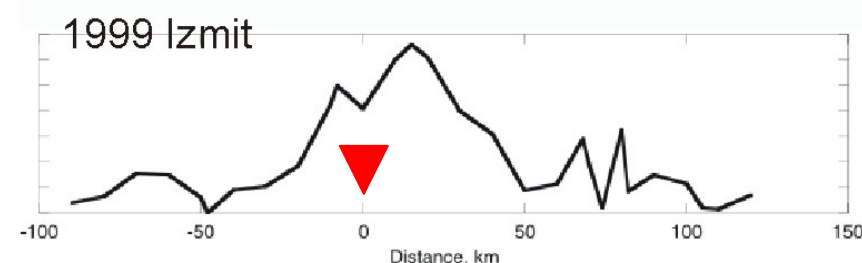
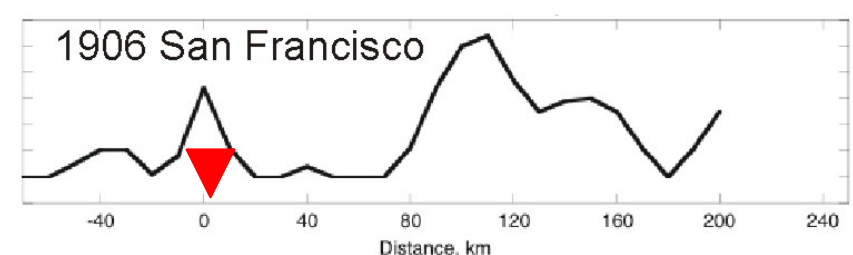
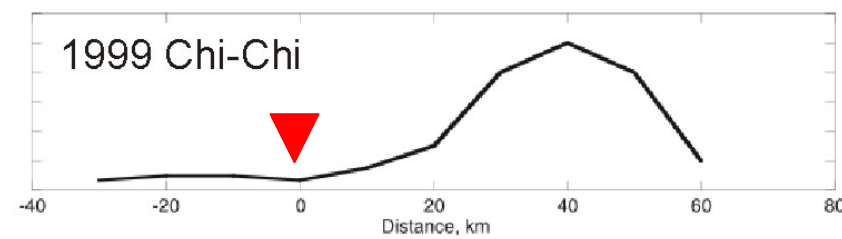
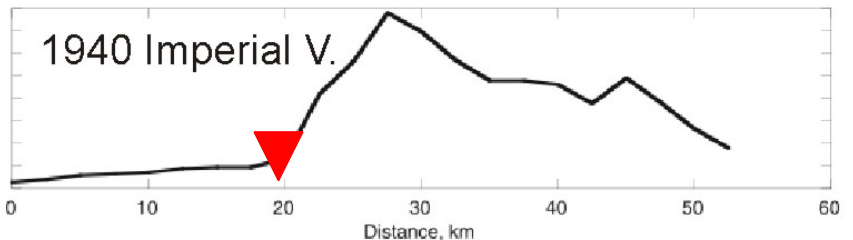
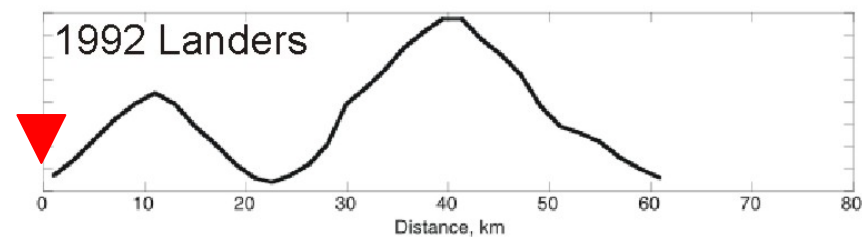
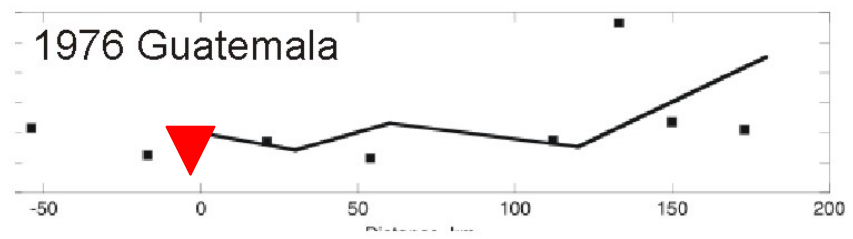
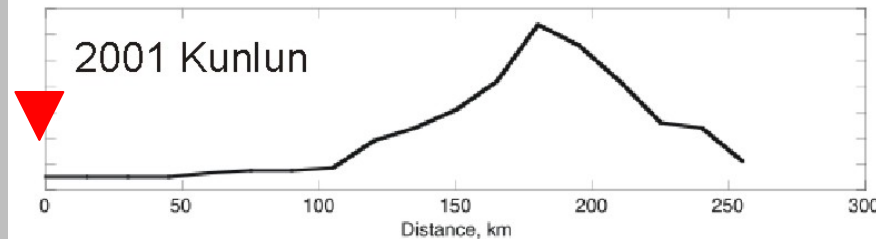
Direct evidences:

- 1) Shallow geometrical complexity observed at all scales (*Tchalenko and Ambrases, 1970; Aydin, 1978; Okubo and Aki, 1987; Aviles et al., 1987; Reches, 1988; Davy, 1993; Johnson et al., 1994*);
- 2) Profilemetry measurements along exumed fault surfaces (*Brown and Scholz, 1985; Power et al., 1988; Power and Tullis, 1991; Brown, 1995*);
- 3) Long – range property fluctuations in geophysical logs (*Hewett, 1986; Leary, 1991*).

Indirect evidences:

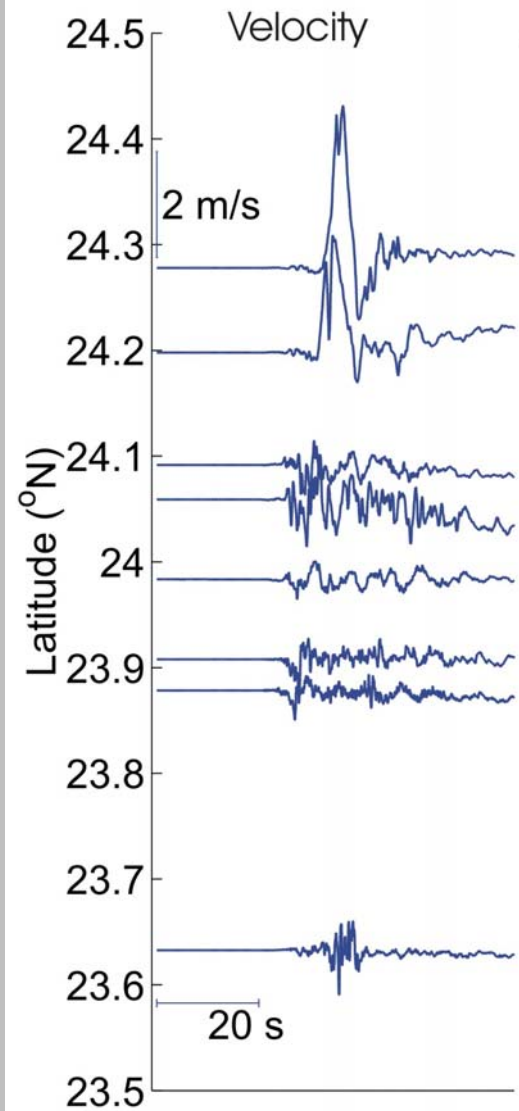
- 1) Complex distribution of earthquake hypocenters (*Kagan, 1994*) and of size and repeated time of earthquake occurrence;
- 2) Presence of abundance of incoherent high – frequency seismic radiation from earthquake rupture zones (*Hanks and McGuire, 1981; Papageorgiou and Aki, 1983; Joyner and Boore, 1988; Stevens and Day, 1994*);
- 3) Short risetimes in earthquake slip histories (*Heaton, 1990; Wald, 1992*);
- 4) Stress drop fluctuations in small events (*Guo et al., 1992; Abercrombie and Leary, 1993; Hough and Dreger, 1995*).

Slip distribution of large earthquakes

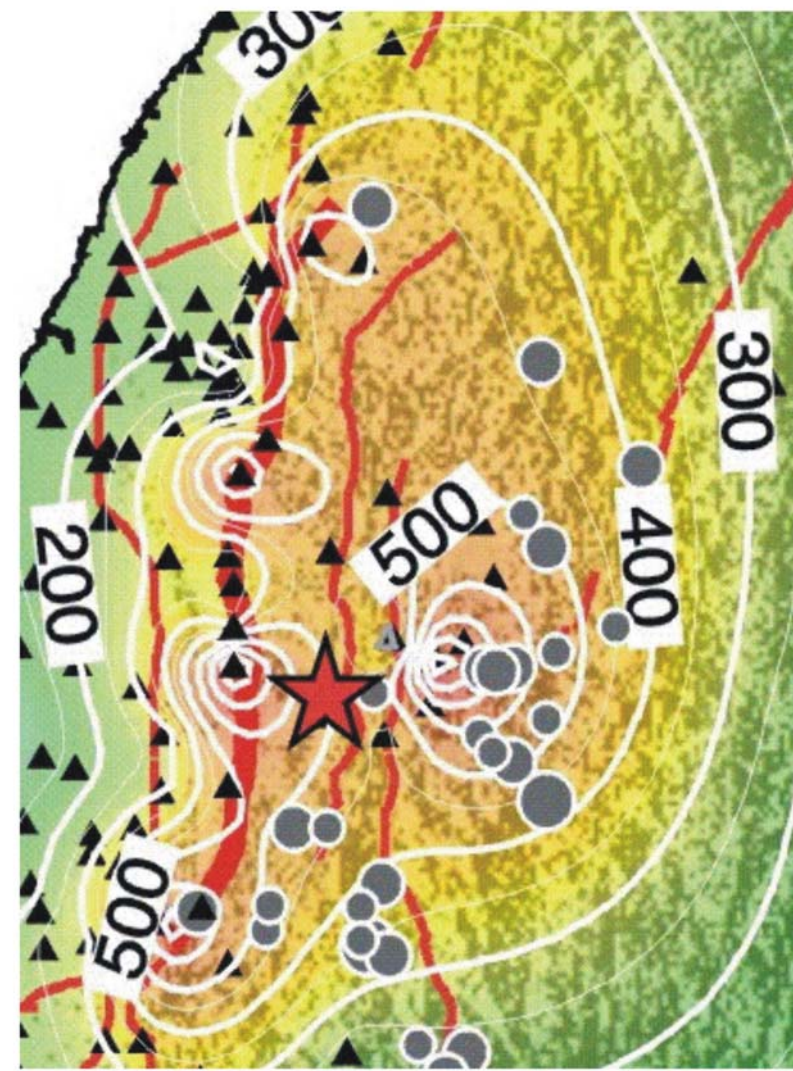


Ground motion from Chi – Chi, Taiwan, EQ

Brodsky and Kanamori (2001)



Ma et al. (1993)





Effects of Strength Heterogeneity #1

i

Slip_var10ani_sw_total

$$S_3 = 0.8$$

$$S_2 = S_1 = 3.0$$

$$\text{In. rake} = 0.785398 \text{ rad.}$$

Anim_Slip_var10ani_sw_total.avi



Homogeneous

Rakediff_26ani_sw

$$S = 0.8$$

In. rake = 0.785398 rad.

Anim_Rakediff_26ani_sw_total.avi

Heterogeneous

Rakediff_var10ani_sw

$$S_3 = 0.8$$

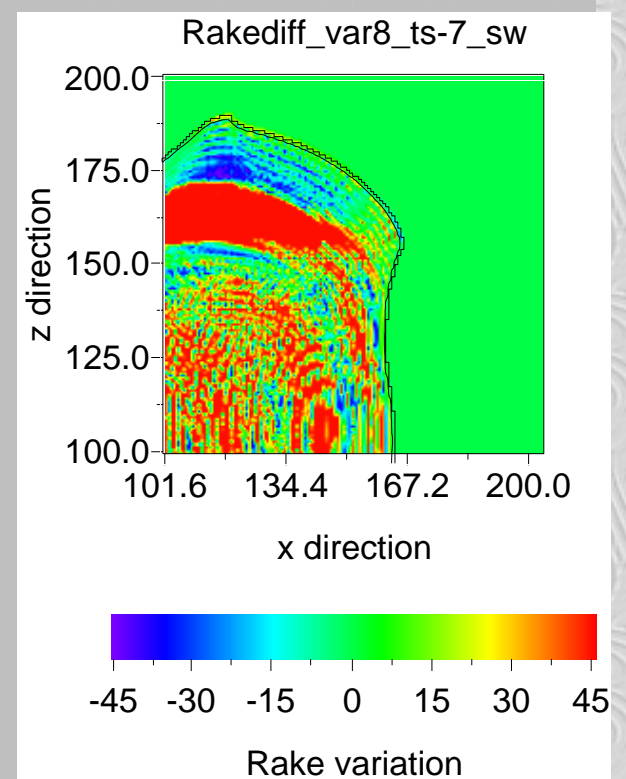
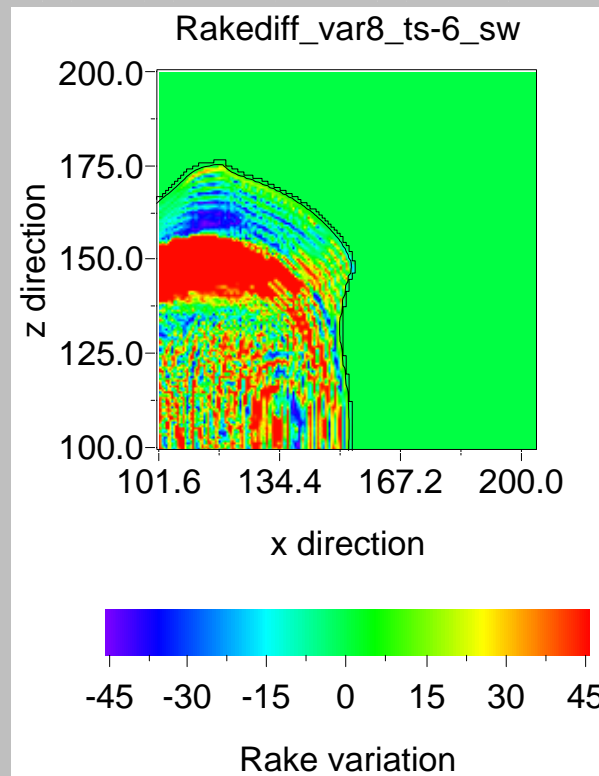
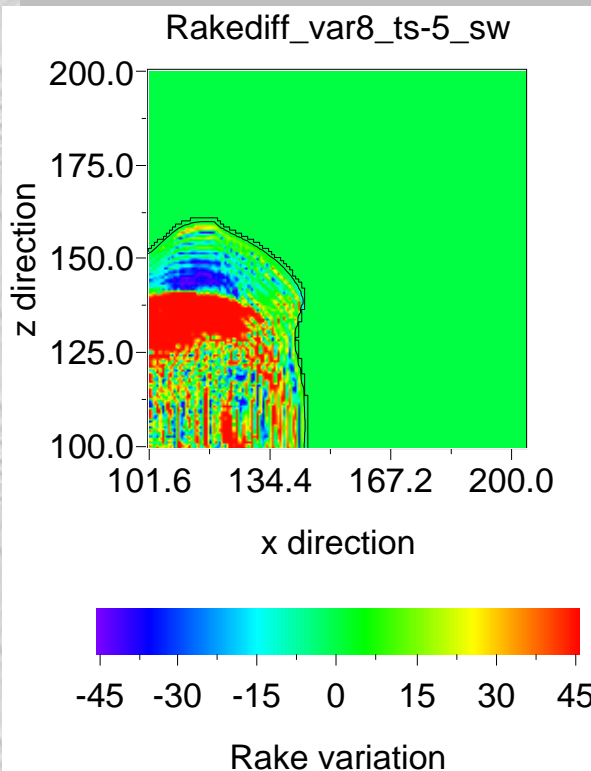
$$S_2 = S_1 = 3.0$$

In. rake = 0.785398 rad.

Anim_Rakediff_var10ani_sw_total.avi

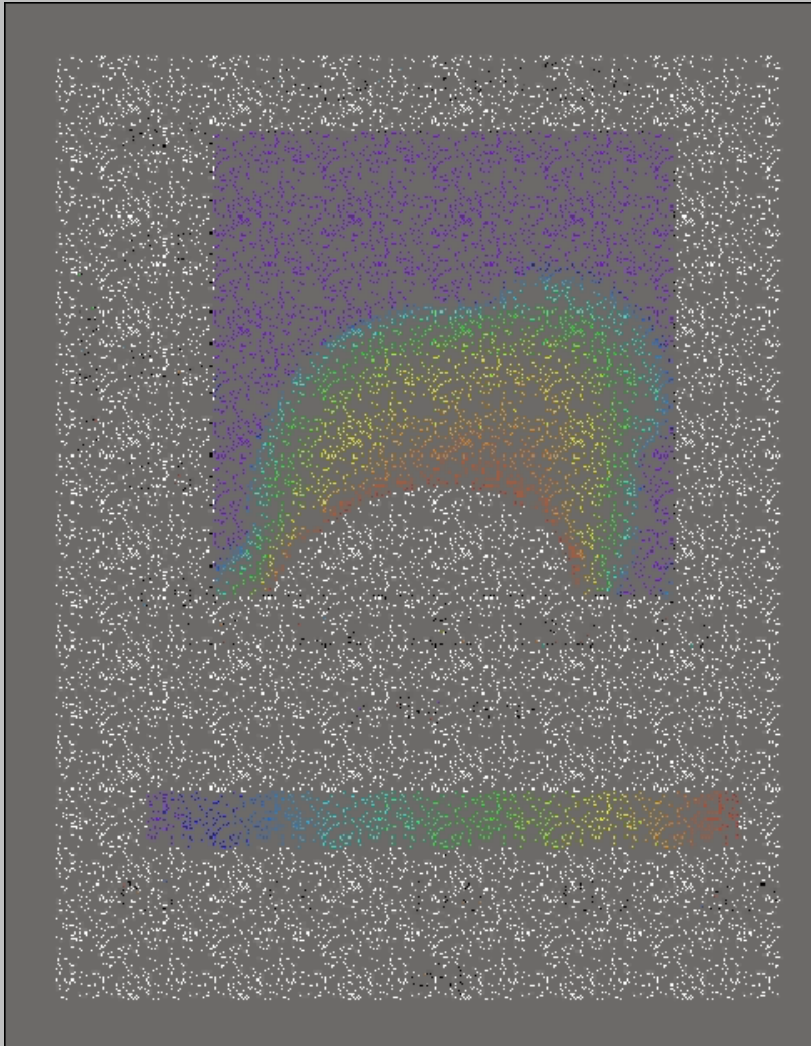


Effects of Strength Heterogeneity #2



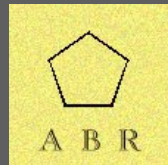


Effects of Free Surface



Anim_Slip_37ani_sw_total.avi

This slide is empty intentionally.



Support Slides: Parameters, Notes, etc.

To not be displayed directly. Referenced above.

Why “truly” 3 – D ?

Remembering the dimensionality d' of the problem:

2 – D Mode II (pure in – plane): $\mathbf{u} = (u_1(x_1, t), 0, 0)$

2 – D Mode III (pure anti – plane): $\mathbf{u} = (0, u_2(x_1, t), 0)$

3 – D Mixed mode: $\mathbf{u} = (u_1(x_1, t), u_2(x_1, t), 0)$

3 – D having only one non null component: $\mathbf{u} = (u_1(x_1, x_2, t), 0, 0)$

Truly 3 – D: $\mathbf{u} = (u_1(x_1, x_2, t), u_2(x_1, x_2, t), 0)$



Test #	26ani_sw	3 - D	FD
Constitutive law	Slip - weakening		
Simulation Date	14-12-02		
System	Mk		
Categorized as	Homogeneous		
Input Set type	<i>Non - dimensional units</i>		
Δx , Δy , Δz	0.2	0.2	0.2
Arrays size	254	83	251
Iterations in time	350		
Mass density (ρ)	1.		
v_s , v_p	1.	1.732	
Initial stress (τ_0)	1.		
Yield stress (τ_u)	1.8		
Frictional level (τ_f)	0.		
Strength (S)	0.8		
Characteristic length (d_0)	1.3	1.3	1.3
Normal stress (σ_n)	1.		
Initial rake	0.785398 rad.		
Initial slip velocity	0.5		
Nucleation point	25.4	25.	
Fault type	<i>Vertical Strike - slip</i>		



Test #	37ani_sw	3 - D	FD
Constitutive law	Slip - weakening		
Simulation Date	15-10-02		
System	<i>Mk</i>		
Categorized as	Homogeneous		
Input Set type	<i>Non - dimensional units</i>		
Δx , Δy , Δz	0.2	0.2	0.2
Arrays size	254	83	251
Iterations in time	350		
Mass density (ρ)	1.		
v_s , v_p	1.	1.732	
Initial stress (τ_0)	1.		
Yield stress (τ_u)	1.8		
Frictional level (τ_f)	0.		
Strength (S)	0.8		
Characteristic length (d_0)	1.3	1.3	1.3
Normal stress (σ_n)	1.		
Initial rake	0.785398 rad.		
Initial slip velocity	0.5		
Nucleation point	25.4	25.	
Fault type	<i>Vertical Strike - slip</i>		



Test #	var10ani_sw 3 - D		
Constitutive law	Slip - weakening		
Simulation Date	19-12-02		
System	<i>Mk</i>		
Categorized as	Heterogeneous		
Input Set type	<i>Non - dimensional units</i>		
Δx , Δy , Δz	0.8	0.2	0.8
Arrays size	254	83	251
Iterations in time	700		
Mass density (ρ)	1.		
v_s , v_p	1.	1.732	
Initial stress (τ_0)	1.	1.	1.
Yield stress (τ_u)	1.8	4.	4.
Frictional level (τ_f)	0.	0.	0.
Strength (S)	0.8	3.	3.
Characteristic length (d_0)	1.3	1.3	1.3
Normal stress (σ_n)	1.		
Initial rake	0.785398 rad.		
Initial slip velocity	0.5		
Nucleation point	25.4	10.	
Fault type	<i>Vertical Strike - slip</i>		



Test #	var8_sw	3 - D	FD
Constitutive law	Slip - weakening		
Simulation Date	08-11-02		
System	Mk		
Categorized as	Heterogeneous		
Input Set type	Non - dimensional units		
Δx , Δy , Δz	0.8	0.2	0.8
Arrays size	254	83	251
Iterations in time	700		
Mass density (ρ)	1.		
v_s , v_p	1.	1.732	
Initial stress (τ_0)	1.	1.	1.
Yield stress (τ_u)	1.8	3.	3.
Frictional level (τ_f)	0.	0.	0.
Strength (S)	0.8	2.	2.
Characteristic length (d_0)	1.3	1.3	1.3
Normal stress (σ_n)	1.		
Initial rake	0.785398 rad.		
Initial slip velocity	0.5		
Nucleation point	25.4	10.	
Fault type	Vertical Strike - slip		